

Research Article

Intercell Radio Resource Management through Network Coordination for IMT-Advanced Systems

Young-June Choi,¹ Narayan Prasad,² and Sampath Rangarajan²

¹ School of Information and Computer Engineering, Ajou University, Suwon 443-749, Republic of Korea

² NEC Laboratories America, Princeton, NJ 08540, USA

Correspondence should be addressed to Young-June Choi, choiyj@ajou.ac.kr

Received 12 January 2010; Accepted 8 July 2010

Academic Editor: Mohammad Shikh-Bahaei

Copyright © 2010 Young-June Choi et al. This is an open access article distributed under the Creative Commons Attribution License, which permits unrestricted use, distribution, and reproduction in any medium, provided the original work is properly cited.

In IMT-Advanced systems, a cross-layer approach coupling network coordination and radio resource managements enables mitigation of intercell interference and throughput improvement of cell-edge users. To facilitate coordination among base stations, we propose a new radio-resource management framework where cell-edge users and cell-interior users are separately managed by two different radio-resource managers. In the proposed framework, we address the issue of how to classify a user as cell-edge user or cell-interior user, and how much radio resource the cell-edge users may occupy. We present a solution where a user switches the user type so as to maximize overall network throughput subject to the condition that their own throughput does not decrease upon switching. We verify our solution using analysis and simulation experiments where two or three BSs are coordinated to support fractional frequency reuse or macrodiversity and demonstrate that our solution can guarantee superior cell-edge performance and achieve a high network throughput.

1. Introduction

Recent developments in the area of wireless communications have witnessed a remarkable proliferation of wireless technologies. While 3G and *Beyond 3G* cellular systems are still being deployed, the IMT-advanced standards have set a goal for an evolutionary growth towards 4G wireless networks. The potential candidate technologies for 4G networks include 802.16m (WiMAX) and LTE-Advanced (3GPP). These next-generation systems have adopted orthogonal frequency division multiple access (OFDMA) as the air-interface technology. In OFDMA systems, as neighboring cells can reuse the same frequency, intercell interference is an important problem that needs to be solved. Due to intercell interference, *cell-edge users* may suffer low data rates (or high error rates) even when the most robust modulation and coding techniques are used.

To enhance the performance of cell-edge users in OFDMA systems, frequency reuse techniques between neighboring cells, have been developed. A simple technique is to exploit a large frequency reuse factor such as 3. With a reuse factor of one, all cells use all frequencies in which

case the intercell interference would be the highest. but cell throughput is greatly reduced because each cell now can use only 1/3 of the total available frequencies (channels). An enhanced reuse technique is to use two reuse factors simultaneously; for example, cell-edge users are supported by a reuse factor of 3 while the others use a reuse factor of 1 [1]. These methods, however, limit flexibility in terms of radio-resource utilization and cell deployment. For flexibility, dynamic channel allocation has been widely examined (see [2, 3] and references therein). In [2], dynamic channel allocation is realized at both a radio network controller (RNC) and at a BS which assign channels at the super-frame level and frame-level, respectively. Dynamic channel allocation is also referred to as dynamic fractional frequency reuse (FFR) [4], and it is known that FFR can enhance cell-edge throughput by about 15% [5] but at the expense of a reduced average cell throughput.

Another technique to enhance cell-edge user performance is macrodiversity. With macro-diversity, multiple BSs can serve a user, thus making the link condition of cell-edge users more reliable and robust [6]. Such a technique has already been adopted in the IEEE 802.16 family of

standards but the current macro-diversity schemes limit the signaling formats (or space-time codes) that can be employed by the coordinated BSs. An emerging technique that is still in its infancy but has nevertheless generated enough interest, is that of network MIMO. The concept of network MIMO (a.k.a. multi-BS MIMO) to perform joint MIMO transmission and reception between multiple coordinated BSs and multiple users over the same radio resources [7, 8]. Network MIMO can be further divided into closed-loop network MIMO, where coordinated BSs have access to and exploit fast changing channel state information to serve multiple users, or open loop network MIMO where only average channel quality information is used to serve the users. Note that open-loop network MIMO subsumes macro-diversity schemes as special cases. In this paper we present our solution to classify users by assuming a simple macro-diversity scheme but our techniques can be readily extended to other more general open-loop network MIMO schemes.

Both dynamic FFR and macro-diversity require coordinated RRM between neighboring BSs within the network. We use RRM to refer to both radio resource management and radio resource managers. If dynamic FFR is deployed in the system, designated neighboring BSs of a cell to which a certain cell-edge user is attached should avoid concurrent transmission over the same set of channels. If macro-diversity is used, one or more neighboring BSs should serve a certain cell-edge user at the same time; this means concurrent transmissions over the same set of channels from multiple BSs to the same user is required. To handle such requirements, the system needs network-level coordination of radio resources through a cross-layer approach between the network level and the radio level. In this paper, we consider two different backhaul network architecture options (hierarchical and flat) and develop a framework for network-assisted RRM within these architectures so as to maximize network throughput and enhance edge-user throughput.

In a conventional cellular architecture, network-level coordination is easier to achieve as radio resources are managed by an upper-level entity such as an RNC. For example, as seen in [2], techniques such as dynamic FFR and macro-diversity can be managed more easily at an RNC since they required coordination among multiple BSs. However, there are other techniques such as channel-aware opportunistic scheduling [9–11] and closed-loop MIMO operations that require real-time channel feedback from users [12]. Wireless channel characteristics, specifically for mobile users, fluctuate due to channel fading, and thus it is required that channel feedback be delivered within one slot/frame (5 msec in WiMAX systems and 1.67 msec in cdma2000 EV-DO/HDR systems) duration [11]. In this case, if RRM is implemented at a central entity, the two-hop delivery of feedback information from a mobile station to the upper-level entity through the BS may make this information outdated and not usable.

In HDR and HSDPA systems [13, 14], where opportunistic scheduling based on channel feedback plays a key role in enhancing cell throughput; user and channel scheduling is performed at the BSs. These systems do not implement

either dynamic FFR or macro-diversity both of which require network-level coordination and are at odds with implementing RRM functions at the BSs. In upcoming 4G systems where techniques such as dynamic FFR and macro-diversity are expected to be deployed together with conventional techniques such as opportunistic scheduling and closed-loop MIMO, it becomes imperative that a framework for RRM be developed to enable such coexistence.

In this paper, we propose a *two-level RRM* framework. We advocate the coexistence of two RRM entities, an upper-level RRM and a lower-level RRM, within the backhaul architecture that connects the BSs. We separate users attached to a BS into two groups; one group consists of users who are classified as cell-edge users and the other consists of users who are classified as cell-interior users. The RRM functions for cell-edge users are handled by the upper-level RRM whereas those for cell-interior users are handled by the lower-level RRM. In a hierarchical backhaul architecture, we expect the upper-level RRM to be deployed at the RNC whereas in a flat backhaul architecture, each BS will deploy both the upper and lower-level RRMs. In the latter case, the upper-level RRM deployed within a BS will coordinate the RRM of an attached cell-edge user with upper-level RRMs deployed at neighboring BSs.

The classification of cell-edge and cell-interior users are *not* based purely on geographic location as in conventional frequency reuse techniques. We classify users as cell-edge or cell-interior users with the goal of maximizing network throughput subject to the condition that the user throughput does not decrease upon switching; for example, a user at the edge of a cell may still get classified as a cell-interior user if such classification leads to higher network throughput with no attendant loss in the user throughput or conversely if such classification increases the user throughput without a loss in the network throughput, this can happen due to the multiuser diversity gain which is obtained when channel-dependent scheduling is employed to serve cell interior users. Furthermore, we also show that as compared to a switching scheme which only aims to maximize the network throughput, our classification scheme results in a better cell-edge performance without a loss in network throughput. Within the proposed framework, we address three main problems: (1) initial user classification, (2) strategy to switch users from one class to another subsequently, and (3) radio-resource reservation in neighboring cells for users who are classified as cell-edge users. We develop solutions for these problems in situations where dynamic FFR and macro-diversity mechanisms are available to cell-edge users. As discussed earlier, these mechanisms require radio resources from multiple neighboring cells.

The remainder of this paper is organized as follows. In Section 2, we provide a brief overview of the current framework for RRM support within a conventional 3G cellular network architecture, which is hierarchical, as well as a Beyond 3G system such as 802.16e (WiMAX) which is flat. In Section 3, we describe the proposed two-level framework for RRM and show its applicability within both a hierarchical architecture and a flat architecture; 4G systems are expected to implement the latter. The framework uses an upper-level

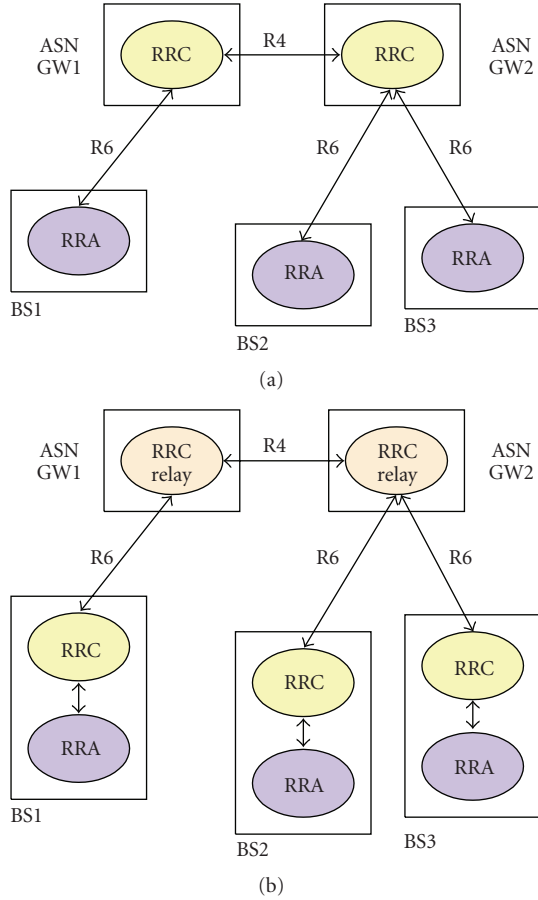


FIGURE 1: Access networks in WiMAX systems: (a) profile A, (b) profile C.

RRM and a lower-level RRM to handle cell-edge and cell-interior users, respectively. In Section 4, we introduce metrics for describing a mechanism for classifying users as cell-edge and cell-interior users, and explain initial user classification. In Section 5, we provide algorithms for switching a user between these two classes. In Section 7, simulation results demonstrate that our classification algorithms improve cell-edge performance. Section 8 provides conclusions from our work.

2. Current RRM Framework

Traditionally, 2.5G and 3G cellular networks have employed a hierarchical backhaul structure. Recently, Beyond 3G and 4G systems such as 802.16e and 802.16m (WiMAX) have been evolving more towards a flat architecture. The WiMAX standard has defined three different profiles for an access service network (ASN) which is the backhaul network that connects multiple BSs to an ASN gateway [15]. In Profile A, which is now defunct, most radio resources are managed by the ASN gateway as in traditional cellular networks and thus has a hierarchical structure. In Profile B, the functionalities of a BS and an ASN gateway are collocated on the same platform/solution, which makes the architecture flat. Profile

C also defines a flat architecture where all the RRM functions are performed at the BS.

Figure 1 presents the WiMAX ASN models for Profiles A and C. In both cases, the interface (named R6) between an ASN gateway and a BS is explicitly defined. In both these profiles, a BS implements a *RRA* (radio resource agent), the difference being where the *RRC* (radio resource controller) is located. A RRA collects information on radio resources and supervises the MAC and PHY functions including power control. A RRC collects radio resource information from RRAs and performs RRM. In Profile A, the RRC is located at the ASN gateway whereas in Profile C, it is co-located with the RRA at the BS; Profile C does support a *RRC relay* at the ASN gateways to relay RRM messages that allows for inter-profile RRM signaling between ASNs that are of type Profile A, B, or C.

In the next section, we will use the WiMAX ASN architecture for Profiles A and C to motivate our two-level RRM framework for a hierarchical architecture and a flat architecture, respectively.

3. Proposed RRM Framework

3.1. Hierarchical Architecture. For a hierarchical backhaul network architecture we propose that upper-level RRM that manages cell-edge users be implemented at the ASN gateway and lower-level RRM that manages cell-interior users be implemented at the BSs. In this way, RRM functionality is distributed between the ASN gateway and the BSs. The motivation for this is as follows. As we discussed in an earlier section, mechanisms such as fractional FFR and macro-diversity require network-level coordination and an ASN gateway is the appropriate place to manage users which are cell-edge users and would benefit from these techniques. Similarly, cell-interior users are most benefited by mechanisms such as channel-aware scheduling and closed-loop MIMO both of which require real-time channel feedback information which are available at the BS; thus, lower-level RRM is best located at the BSs. Of course, our proposal requires that cell-edge and cell-interior users be classified appropriately, and this classification procedure is discussed in the next sections.

Since the cell-interior users are controlled by BSs, ASN gateways can relay data to/from those users without performing any RRM function. The cell-edge users are controlled by ASN gateways and in this case the BSs can relay data to/from those users without performing any RRM function. In addition to RRM functions for the appropriate set of users, common functions for all users at Layer 1 and Layer 2 are performed at the BSs and Layer 3 functions are performed at the ASN gateway.

Figure 2 presents our proposal implemented within a WiMAX system. In addition to the RRC (found in a Profile A ASN-gateway), we also require an RRC relay at the ASN gateway (similar to one found in a Profile C ASN-gateway). The RRC at the ASN-gateway implements the upper-level RRM functionality and controls the RRA at the BS to manage cell-edge users. The RRC-relay allows

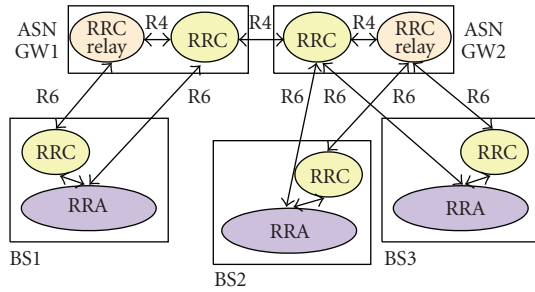


FIGURE 2: The proposed access network applied to WiMAX systems.

communication between two RRCs that are each located at the BSs. These RRCs at the BS implement the lower-level RRM and communicate with the local RRA to manage the cell-interior users. Note that RRCs in ASN gateways communicate directly with each other to manage cell-edge users who are the most likely to move across different ASN gateways.

Now that we have discussed our two-level RRM framework with respect to WiMAX architectures, we will henceforth use the terms upper RRC and lower RRC to denote a generic upper-level RRM and a lower-level RRM, respectively.

3.2. Flat Architecture. A two-level RRM framework can be implemented within a flat backhaul network architecture as well. Because there is no central coordinator to coordinate the BSs (such as an ASN gateway), each BS handles both its cell-edge users and cell-interior users; that is, an upper RRC and a lower RRC coexist at each BS. Each cell-edge user will have a serving BS to which it is attached that plays the role of a coordinator; these users are managed in a decentralized manner. Figure 3 illustrates implementation for upper and lower RRCs within a flat architecture. Using a negotiation protocol, a BS can designate a resource zone which is reserved for the cell-edge users that it coordinates with its neighboring BSs. This resource-zone specifies the different radio resources within the cell controlled by this BS that are a priori reserved to be used only by cell-edge users. When a cell-interior user changes classification to a cell-edge user, the serving BS will request reservation of radio resources for this user to the neighboring BSs. If the neighboring BSs are able to allocate enough resources, the user will be reclassified. The overall operation will be the same as in the hierarchical architecture, except the upper RRCs at neighboring BSs have to coordinate with one another to handle cell-edge users.

Therefore, we develop an algorithm of deciding whether a user will be served by an upper RRC or a lower RRC, which is applicable regardless of network architecture.

3.3. Radio Resource Management. In the proposed framework, both cell-edge and cell-interior users share radio resources. This sharing can be enabled through a simple mechanism where cell-edge users use radio resources first and the cell-interior users use the residual radio resources. This mechanism can be implemented, for example in

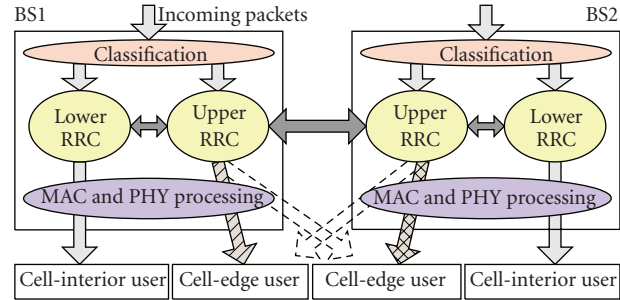


FIGURE 3: Downlink transmission in our flat architecture.

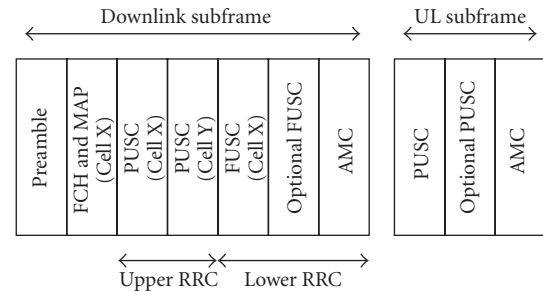


FIGURE 4: OFDMA frame with multiple zones in IEEE 802.16 systems. In our proposed architecture, PUSC and FUSC are assigned to upper RRC and lower RRC, respectively, over downlink and subcarriers are orthogonally allocated to cell X and cell Y.

the WiMAX standards, using existing frame structure. In a WiMAX (802.16e, 802.16m) system, the upper RRC can write the downlink and uplink maps by allocating subcarriers to cell-edge users first, and then the lower RRC can write the residual map for cell-interior users. This is implementable by the concept of multiple zones. IEEE 802.16 systems define multiple zones where each zone is able to support PUSC (partial usage of subcarriers), FUSC (full usage of subcarriers), and AMC (adaptive modulation and coding) modes, as shown in Figure 4. These zones can now be used by upper RRC and lower RRC to assign radio resources to cell-edge and cell-interior users, respectively. For example, the PUSC mode can be used orthogonally by cell-edge users whereas the FUSC or AMC mode can be used by cell-interior users.

One concern is that an upper RRC could monopolize radio resources available at a certain BS, thus starving its cell-interior users. To avoid this, we could restrict the total amount of zone/resource (e.g., number of subcarriers) that an upper RRC can occupy. More dynamically, radio resources can be adjusted according to a negotiation protocol between upper and lower RRCs, and it is also feasible to design an interactive RRM algorithm between both entities. The upper RRC may take into account the amount of data to be served at the lower RRC, or vice versa. Detailed protocols for such negotiation are beyond the scope of this paper.

In the next sections, we first discuss a classification algorithm for grouping users into cell-edge and cell-interior

users. Following that, we develop an algorithm to dynamically determine when a user should be reclassified. To implement the initial classification algorithm, classifiers that allocate a user to either an upper RRC or a lower RRC have to be located at the ASN gateways or at the BSs in the hierarchical architecture or flat architecture, respectively. These classifiers determine the classification of new users as well as the reclassification of existing users.

4. Initial User Classification and Metrics

In this section, we introduce metrics for classifying a user as a cell-edge user to be assigned to an upper RRC and also describe the initial classification of a new user.

4.1. Computation of User Capacities. We would like to determine the capacity a user can achieve when it belongs to the lower RRC (cell-interior user group) or an upper RRC (cell-edge user group). For simplicity, we suppose that a user is able to measure their average signal-to-interference-plus-noise ratio (SINR) as well as the average signal strengths from one dominant neighboring BS and their serving BS, respectively. In the following, we only deal with the case where a cell-edge user is served by at most two BSs, since it is easy to extend the analysis to the case where three or more BSs can serve the user.

4.1.1. Capacity of Cell-Interior Users. Consider a specific lower RRC user in cell 1 and assume that it is served only by BS 1 without any cooperation by neighboring BSs. Let C_1 denote the resulting downlink capacity per unit resource and let S_1 denote the average received signal strength from BS 1 at the user of interest. Further, let the dominant interfering neighboring BS be indexed by 2 with I_2 denoting the average received signal strength from BS 2 at the user of interest. Next, let I_o be the average interference to the user (which is in cell 1) generated by neighboring BSs other than BS 2 and let N be thermal noise variance. Then, the average received SINR of the user is given by $S_1/(I_2 + I_o + N)$. C_1 is a function of this average SINR, and can be computed as

$$C_1 = \log\left(1 + \frac{S_1}{I_2 + I_o + N}\right). \quad (1)$$

Letting $\gamma_1 = S_1/(I_o + N)$ and $\gamma_2 = I_2/(I_o + N)$, we can rewrite C_1 as

$$C_1 = \log\left(1 + \frac{S_1}{\gamma_2(I_o + N) + I_o + N}\right) = \log\left(1 + \frac{\gamma_1}{\gamma_2 + 1}\right). \quad (2)$$

Note that the average SINR here is a function of the distance-dependent path-loss and possibly large-scale shadow fading but not of the small scale fading which changes on a much finer time scale and is assumed to be averaged out.

4.1.2. Capacity of Cell-Edge Users. Now consider two cases where the cell-edge users are supported by, (a) fractional frequency reuse, and (b) macro-diversity. In each case, no

opportunistic scheduling is employed and the users are assigned rates based on their average SINRs.

- (a) Dynamic FFR—in this case, to mitigate the interference from a dominant neighboring cell at a particular cell-edge user, the two BSs (serving BS as well as the dominant interfering BS) are coordinated such that the dominant neighboring BS will not use a certain quantity of resources that is allocated to the cell-edge user. As interference from the neighboring BS is eliminated, the user can achieve a better capacity. In particular, in the above example, I_2 is removed so the user's capacity achieved by the cooperation of BSs 1 and 2 via FFR, denoted by $C_{1,2}$, is expressed as

$$C_{1,2} = \log\left(1 + \frac{S_1}{I_o + N}\right) = \log(1 + \gamma_1). \quad (3)$$

- (b) Macro-diversity—we consider Alamouti's space-time coding [16] for supporting downlink macro-diversity. That is, the serving BS and the dominant neighboring BS transmit two signals γ_1 and γ_2 at the same time over the same frequency band, followed by $-\gamma_2^*$ and γ_1^* . The transmissions from the two BSs can be coherently combined using a simple receiver [16]. Then, if the user is served by an upper RRC for macro-diversity, their capacity will be given by

$$C_{1,2} = \log\left(1 + \frac{S_1 + I_2}{I_o + N}\right) = \log(1 + \gamma_1 + \gamma_2), \quad (4)$$

Obviously, $C_{1,2}$ in the two cases is higher than C_1 given in (1), but some amount of resource from BS 2 needs to be additionally provisioned for this user. It is possible to obtain orthogonal space-time codes for three transmit antennas, which in our case correspond to the antennas at the three neighboring BSs. From [17], it can be inferred that the resulting capacity is given by

$$C_{1,2,3}(k) = \frac{3}{4} \cdot \log\left(1 + \frac{S_1 + I_2 + I_3}{I'_o + N}\right). \quad (5)$$

where I_2 and I_3 are the received signal strengths from two neighboring BSs, and I'_o is the interference from neighboring BSs other than those two BSs.

4.2. Computation of Throughput. The throughput of a cell-interior user i in cell x is denoted by $T_x(i)$ and it can be expanded as $T_x(i) = \alpha(i)C_x(i)$, where $C_x(i)$ denotes the average capacity of the interior user i in cell x . $\alpha(i)$ denotes the average ratio of resource allocated to user i (e.g., the average ratio of slots or quantity of resource in the frequency and time domains). Similarly, the throughput of a cell-edge user i managed by the cooperation of BS x and BS y is denoted by $T_{x,y}(i)$ and it can be expanded as $T_{x,y}(i) = \alpha(i)C_{x,y}(i)$, where the average capacity $C_{x,y}(i)$ can be computed as in (3) or (4) depending on whether FFR or macro-diversity is employed. Note that each cell expends a fraction of its available resources to serve the cell-edge users.

The assignment of α 's relies on a scheduling policy employed at the BSs. We do note that while user k is managed by the lower RRC, $\alpha(k)$ may be adjusted by the scheduling policy used or by the reclassification of other users. On the other hand, the ratio α for a cell-edge user is determined when the user is admitted into the network as a cell-edge user or when the user is switched from the lower RRC to the upper RRC. This computation will be illustrated in the sequel. However, we assume $\alpha(k)$ to be a constant value while user k is being managed by the upper RRC. This simplifying assumption is made because resource rearrangement for such users entails complex calculation involving all the combinations of pairs of neighboring BSs. To summarize, $\alpha(k)$ changes in the following cases.

- (i) $\alpha(k)$ can decrease, if user k is managed by the lower RRC and a new user requiring the cell resource arrives.
- (ii) $\alpha(k)$ can increase, if user k is managed by the lower RRC and some resource is freed due to the departure of an existing user who occupied the cell resource.
- (iii) $\alpha(k)$ can increase or decrease, if user k switches the serving RRC from a lower RRC to an upper RRC, or vice versa.
- (iv) Besides, $\alpha(k)$ is forced to change by a hand-off that occurs regardless of the classification of the user.

Let β_x be the ratio of resource in cell x allocated for cell-edge users. β_x can then be expressed as

$$\beta_x = \sum_{y \in V_x} \sum_{i \in U_{x,y}} \alpha(i), \quad (6)$$

where $U_{x,y}$ is the set of cell-edge users which are managed by the cooperation of BSs x and y , and V_x is the set of BSs which cooperate with BS x (i.e., its neighboring BSs). BS x will use the remaining resource $1 - \beta_x$ for its cell-interior users. We further assume that $\beta_x \leq \beta_{\max}$ in order to avoid monopolization of the resources by the upper RRC.

4.3. Initial User Classification. A new user is admitted to the system as a cell-edge or a cell-interior user. We consider a simple scheme that guarantees a minimum throughput $T_{\min}(i)$ given by user i 's QoS requirement

$$T_x(i) \geq T_{\min}(i); \quad T_{x,y}(j) \geq T_{\min}(j), \quad \forall x, y, i, j. \quad (7)$$

The capacity of a new user n , $C_x(n)$, upon admission as a cell-interior user in cell x is first estimated. Similarly, the capacity $C_{x,y}(n)$ of the user upon admission as a cell-edge user served by BSs x and y is also computed using (3) or (4). Then, the user can be admitted as a cell-interior user by BS x only if its minimum throughput requirement can be met, that is, only if

$$\sum_{i \in L_x} \frac{T_{\min}(i)}{C_x(i)} + \frac{T_{\min}(n)}{C_x(n)} \leq 1 - \beta_x - \delta, \quad (8)$$

where L_x is the set of cell-interior users in cell x and δ is a margin for absorbing the change of some users' average

capacities or accepting hand-off users; for our discussion, δ is considered to be a design parameter. If user n is admissible in BS x as a cell-interior user, a ratio $\alpha(n)$ is determined according to the scheduling policy adopted by BS x . Once $\alpha(n)$ is determined, the classifier (or admission controller) checks if there exists an $\alpha'(n)$ acceptable by BSs x and y for some $y \in V_x$ (using our upward RRC switch algorithm in Section 5) which can lead to better system and user throughputs. If such an $\alpha'(n)$ exists, the user is admitted as a cell-edge user which is served by BSs x and y ; otherwise it is admitted as a cell-interior user which is served by BS x .

Notice that in (8), we have implicitly assumed that the throughput of an existing interior user i in cell x does not change upon addition of a new user. However, when channel dependent scheduling is employed, users may achieve a greater throughput due to a larger multiuser diversity gain. Thus, (8) is a conservative condition for admitting a new user. In general, for channel dependent scheduling, the increase in throughput with the addition of a new user or the decrease in throughput with the deletion of another interior user, is small when the number of interior users is sufficiently large (10 or more verified in simulations). Henceforth, in the case of channel dependent scheduling, we will assume a sufficiently large population of interior users in each cell and ignore this change in the average capacity of an interior user.

5. Strategy for User Reclassification

We now derive the condition for reclassifying users and switching them from upper RRC to lower RRC or vice versa. Users that do not satisfy these conditions will, by default, not be reclassified. The objective behind reclassifying users is to maximize the sum throughput over all the users in the network covered by an ASN gateway (or a set of BSs deployed for cooperation) subject to a minimum throughput guarantee for each user. In particular, each user is allocated to either a lower RRC or an upper RRC to meet the following objective:

$$\max \left[\sum_{x \in \mathcal{N}} \sum_{i \in L_x} T_x(i) + \sum_{x,y \in \mathcal{N}} \sum_{j \in U_{x,y}} T_{x,y}(j) \right] \quad (9)$$

$$T_x(i) \geq T_{\min}(i); \quad T_{x,y}(j) \geq T_{\min}(j), \quad \forall x, y, i, j,$$

where \mathcal{N} is the set of BSs within the domain. Further, this reclassification is also subject to the condition that the switching (reclassified) user's throughput must not decrease.

We are now ready to propose our reclassification strategy in which a user is allowed to switch only if both its own throughput as well as the system throughput do not decrease and at-least one of them strictly increases.

5.1. Upward RRC Switch. We first consider an upward RRC switch algorithm, when user k tries to switch their RRC from a lower RRC to an upper RRC. Assume that the user is being served by cell 1 and the current ratio α for the user is $\alpha(k)$.

Suppose that user k 's ratio changes to $\alpha'(k)$ after the RRC switch, when he is supposed to be managed by BSs 1 and 2. User k will accept the RRC change when their throughput becomes higher by changing the RRC, so the first condition for reclassification is

$$\alpha'(k)C_{1,2}(k) - \alpha(k)C_1(k) \geq 0. \quad (10)$$

Since $\alpha'(k)C_{1,2}(k) \geq \alpha(k)C_1(k) \geq T_{\min}(k)$, the condition in (10) will ensure that the minimum throughput requirement will also be satisfied postswitching.

Next, we consider the impact of switching on system throughput which is more involved. In particular, there are three factors that must be accounted for.

(i) *The Throughput Loss in Cell 2.* Notice that user k postswitching will take an additional resource $\alpha'(k)$ from BS 2 which could have been used for other users in that cell if it had not been used for dynamic FFR or macro-diversity. However, it is very hard to precisely estimate this throughput loss since it depends on the cell 2's scheduling rule. Consequently, we use a simple way to quantify this loss as $\alpha'(k) \cdot \bar{C}_2$, where \bar{C}_2 is the average per-user capacity of cell 2's interior users. Note that with our assumption of infinitely backlogged traffic, cell-interior users of any BS will always fully utilize the available resources.

(ii) *The Throughput Change in Cell 1.* The throughput of the current serving cell (cell 1) can change due to switching in the following manner. First, if $\alpha'(k) < \alpha(k)$, the residual part $\alpha(k) - \alpha'(k)$ will be distributed among cell 1's interior users and together they will achieve an average throughput gain of $(\alpha(k) - \alpha'(k)) \cdot \bar{C}_1$, where \bar{C}_1 is the average per-user capacity of cell 1's interior users (excluding user k). Otherwise, that is, if $\alpha'(k) > \alpha(k)$, cell 1's interior users will lose an average throughput of $(\alpha'(k) - \alpha(k)) \cdot \bar{C}_1$. In either case, the net throughput change in cell 1 is expressed by $(\alpha(k) - \alpha'(k)) \cdot \bar{C}_1$.

(iii) *System Constraints.* We must ensure that the switching operation does not violate the minimum throughput requirement of any user or the maximum limit on the resource ratio reserved for cell-edge users in any cell. Specifically, if either $\beta_1 + \alpha'(k)$ or $\beta_2 + \alpha'(k)$ is greater than β_{\max} , or the additional resource $\alpha'(k)$ taken from BS 2 or $\alpha'(k) - \alpha(k)$ taken from BS 1 (when $\alpha'(k) > \alpha(k)$) jeopardizes the minimum allocation for users in L_2 or $L_1 - \{k\}$, user k cannot be allowed to use $\alpha'(k)$ by the upper RRC.

Thus, the first two conditions dictate that a postswitching ratio $\alpha'(k)$ chosen to maximize the network-side throughput in (9), should satisfy

$$\alpha'(k) \left[C_{1,2}(k) - \bar{C}_1 - \bar{C}_2 \right] - \alpha(k) \left[C_1(k) - \bar{C}_1 \right] \geq 0. \quad (11)$$

On the other hand, the system constraints impose that $\alpha'(k)$ should also be constrained to satisfy

$$\begin{aligned} \alpha'(k) &\leq \min \left[\beta_{\max} - \beta_1, \beta_{\max} - \beta_2, \right. \\ &\quad \left. 1 - \beta_1 - \sum_{i \in L_1 - \{k\}} \frac{T_{\min}(i)}{C_1(i)}, 1 - \beta_2 - \sum_{i \in L_2} \frac{T_{\min}(i)}{C_2(i)} \right]. \end{aligned} \quad (12)$$

Thus, the optimal ratio $\alpha'(k)$ can be determined by solving the following optimization problem:

$$\begin{aligned} \max \alpha'(k) \left[C_{1,2}(k) - \bar{C}_1 - \bar{C}_2 \right] - \alpha(k) \left[C_1(k) - \bar{C}_1 \right] \\ \text{subject to (10), (11), and (12).} \end{aligned} \quad (13)$$

The solution for the above objective is given by the following proposition which is proved in Appendix A.

Proposition 1. *The condition of changing a user k 's RRC from a lower RRC to an upper RRC with the cooperation of BSs 1 and 2 is summarized as follows:*

(i) *If $C_{1,2}(k) - \bar{C}_1 - \bar{C}_2 < 0$ and $C_1(k) - \bar{C}_1 < 0$, then switching is allowed only if*

$$\bar{C}_1 \cdot C_{1,2}(k) - (\bar{C}_1 + \bar{C}_2) \cdot C_1(k) \geq 0 \quad (14)$$

and if the postswitching ratio $\alpha(k)C_1(k)/C_{1,2}(k)$ meets the condition (12). The optimal $\alpha'(k)$, when these two conditions are met, is given by

$$\alpha'(k) = \frac{\alpha(k)C_1(k)}{C_{1,2}(k)}. \quad (15)$$

(ii) *If $C_{1,2}(k) - \bar{C}_1 - \bar{C}_2 = 0$ and $C_1(k) - \bar{C}_1 < 0$, $\alpha'(k)$ can be chosen arbitrarily subject to (10) and (12).*

(iii) *If $C_{1,2}(k) - \bar{C}_1 - \bar{C}_2 > 0$ and $C_1(k) - \bar{C}_1 \leq 0$, $\alpha'(k)$ should be the maximal available value subject to (10) and (12).*

The case of $C_{1,2}(k) - \bar{C}_1 - \bar{C}_2 > 0$ and $C_1(k) - \bar{C}_1 > 0$ will be separately mentioned at the end of this subsection.

5.2. Downward RRC Switch. Next, we describe a downward RRC switch algorithm, when user k managed by the upper RRC through cooperation between BSs 1 and 2, tries to switch their RRC to a lower RRC managed by cell 1. Also, let $\alpha(k)$ and $\alpha'(k)$ be the resource ratios before and after the switch, respectively. In order to determine the user's throughput postswitching for a given $\alpha'(k)$, the system can use a capacity $C_1(k)$ which is computed using the average SINR reported by user k had he been an interior user in cell 1.

As in the case of upward RRC switch, user k will accept the RRC switch when their throughput becomes higher by

changing the RRC. Consequently, the first condition for the downward RRC switch is given by

$$\alpha'(k)C_1(k) - \alpha(k)C_{1,2}(k) \geq 0. \quad (16)$$

Next, the impact of the downward RRC switch on the system throughput depends on the following factors.

(i) *The Throughput Gain in Cell 2.* The reclassification of user k will release a ratio $\alpha(k)$ of resource in BS 2 which can be distributed to the cell-interior users in BS 2. Thus, the average sum throughput gain by interior users in cell 2 can be quantified as $\alpha(k) \cdot \bar{C}_2$.

(ii) *The Throughput Change in Cell 1.* Notice that if $\alpha'(k) < \alpha(k)$, the residual part $\alpha(k) - \alpha'(k)$ can be distributed to cell 1's interior users who will together achieve an average throughput gain of $(\alpha(k) - \alpha'(k)) \cdot \bar{C}_1$. Otherwise, that is, if $\alpha'(k) > \alpha(k)$, they will lose an average throughput of $(\alpha'(k) - \alpha(k)) \cdot \bar{C}_1$.

(iii) *System Constraints.* In the case $\alpha'(k) > \alpha(k)$, the additional resource $\alpha'(k) - \alpha(k)$ taken from BS 1 should not jeopardize the minimum throughput requirement of any of its interior users in L_1 .

Therefore, a postswitching ratio $\alpha'(k)$ is acceptable only if it leads to an increase in system throughput, that is, it satisfies

$$\alpha'(k)[C_1(k) - \bar{C}_1] - \alpha(k)[C_{1,2}(k) - \bar{C}_1 - \bar{C}_2] \geq 0, \quad (17)$$

and also respects the system constraints, that is,

$$\alpha'(k) \leq 1 - \beta_1 - \sum_{i \in L_1} \frac{T_{\min}(i)}{C_x(i)}. \quad (18)$$

Thus, the optimal ratio $\alpha'(k)$ can be determined by solving the following optimization problem:

$$\max \alpha'(k)[C_1(k) - \bar{C}_1] - \alpha(k)[C_{1,2}(k) - \bar{C}_1 - \bar{C}_2] \quad (19)$$

subject to (16), (17), and (18).

The solution to the above problem is given by the following proposition. The proof is omitted because it is similar to that of the previous proposition corresponding to the upward RRC switch.

Proposition 2. *The conditions for reclassifying a user k and changing their RRC from an upper RRC to a lower RRC is summarized as follows.*

(i) *If $C_1(k) - \bar{C}_1 < 0$ and $C_{1,2}(k) - \bar{C}_1 - \bar{C}_2 < 0$, then switching is allowed only if*

$$(\bar{C}_1 + \bar{C}_2) \cdot C_1(k) - \bar{C}_1 \cdot C_{1,2}(k) > 0, \quad (20)$$

and if the postswitching ratio $\alpha(k)C_{1,2}(k)/C_1(k)$ meets the condition (18). The optimal $\alpha'(k)$, when these two conditions are met, is given by

$$\alpha'(k) = \frac{\alpha(k)C_{1,2}(k)}{C_1(k)}. \quad (21)$$

(ii) *If $C_1(k) - \bar{C}_1 = 0$ and $C_{1,2}(k) - \bar{C}_1 - \bar{C}_2 < 0$, $\alpha'(k)$ can be chosen arbitrarily subject to (16) and (18).*

(iii) *If $C_1(k) - \bar{C}_1 > 0$ and $C_{1,2}(k) - \bar{C}_1 - \bar{C}_2 \leq 0$, $\alpha'(k)$ should be the maximal possible value subject to (16) and (18).*

Remark 1. The case of $C_1(k) - \bar{C}_1 > 0$ and $C_{1,2}(k) - \bar{C}_1 - \bar{C}_2 > 0$ can be considered in both upward and downward switchings, where $\alpha'(k)$ should be the maximal possible value subject to other constraints. Suppose that user k in cell 1 is served by a lower RRC and satisfies $C_1(k) - \bar{C}_1 > 0$ and $C_{1,2}(k) - \bar{C}_1 - \bar{C}_2 > 0$. Then, if upward switching is permitted, the user will seek a maximal $\alpha'(k)$ subject to the other conditions required for the upward RRC switch. Upon switching, the user will then try to switch to a lower RRC, again seeking a maximal $\alpha'(k)$ subject to the other conditions required for the downward RRC switch. It can be verified that an upward (third) switch will be not possible and the same observation holds if the user were originally served by the upper RRC. Thus, users satisfying $C_1(k) - \bar{C}_1 > 0$ and $C_{1,2}(k) - \bar{C}_1 - \bar{C}_2 > 0$ may switch at most twice, and in our simulation, such users are observed to mainly remain in the lower RRC.

Remark 2. We now justify the extra condition we imposed that a user's throughput must not decrease upon switching, instead of just requiring an increase in system throughput for switching, where the latter will be referred to as *relaxed switching* in the sequel. This additional constraint ensures better cell-edge performance by protecting cell edge users against loss in throughput. Consider the upward switch of a user in cell 1 and assume that an upward switch is possible in relaxed upward switching but not in our switching. In this case, with upward relaxed switching, the system can decide to reclassify an interior user with a lower average capacity as a cell-edge user and allocate a resource ratio just enough to meet its minimum throughput. Moreover, the increase in system throughput in this case is due to an increase in the sum throughput of cell 1's other interior users. A similar observation holds for the downward switch case. Thus, the additional constraint prevents the system from using switching to boost system throughput by starving edge users.

5.3. Simplified Solutions. We now develop simplified solutions for both the RRC switch algorithms when the capacity of an interior user can be computed using (1). We make the assumption that in order to be eligible for switching a user must satisfy $C_1(k) < \bar{C}_1$ as well as $C_{1,2}(k) < \bar{C}_1 + \bar{C}_2$. Note that this assumption is reasonable since the average capacity of a user k at the edge of cell 1 will be smaller than the average per-user capacity of the cell-interior users and is validated in our simulation. As a consequence, only the first cases in both Propositions 1 and 2 are now possible and we address them below.

5.3.1. Fractional Frequency Reuse. Suppose that fractional frequency reuse is employed to support the cell-edge users.

Now consider the upward RRC switch. Using the capacity expression given in (3), the condition in (14) can be expressed as

$$\bar{C}_1 \log(1 + \gamma_1) - (\bar{C}_1 + \bar{C}_2) \log\left(1 + \frac{\gamma_1}{\gamma_2 + 1}\right) \geq 0. \quad (22)$$

The above expression in turn can be compactly written as

$$(1 + \gamma_1)(1 + \gamma_2)^{1+\lambda} \geq (1 + \gamma_1 + \gamma_2)^{1+\lambda}, \quad (23)$$

where $\lambda = \bar{C}_2/\bar{C}_1$. Similarly, it can be shown that the corresponding condition for the downward RRC switch is given by (23) but where the inequality is reversed.

5.3.2. Macrodiversity. Next, when macro-diversity is employed to support the cell-edge users, using the capacity expression given in (4), the condition (14) in the upward RRC switch can be expressed as

$$\bar{C}_1 \log(1 + \gamma_1 + \gamma_2) - (\bar{C}_1 + \bar{C}_2) \log\left(1 + \frac{\gamma_1}{\gamma_2 + 1}\right) \geq 0. \quad (24)$$

This can be further rewritten as

$$(1 + \gamma_2)^{1+\lambda} \geq (1 + \gamma_1 + \gamma_2)^\lambda. \quad (25)$$

The corresponding condition for the downward RRC switch is given by (25) but where the inequality is reversed.

Therefore, in order to decide the RRC switch using the simplified conditions, each user can report γ_1 and γ_2 to the classifier, and the classifier should be able to determine λ . The role of γ_1 , γ_2 , and λ is highlighted in the following proposition.

Proposition 3. *An upward RRC switch requires an increasing value of γ_2 as λ increases, given an arbitrarily fixed γ_1 . Conversely, a downward RRC switch requires a decreasing value of γ_1 as λ increases, given an arbitrarily fixed γ_2 .*

The proof is given in Appendix B.

Figure 5 depicts the boundary conditions of switching a RRC as a function of γ_1 and γ_2 as given by (23) and (25) for fractional frequency reuse and macro-diversity, respectively. As stated in Proposition 3, a greater γ_2 is needed for an upward switch when λ is higher.

Thus far, we have assumed that the average capacity of the interior users in a neighboring cell is available. When this information is unavailable in the network, or each user (instead of a classifier or an admission controller) independently wants to decide the RRC switch without network-level information, we can obtain approximate conditions assuming $\lambda = 1$ (i.e., $\bar{C}_1 = \bar{C}_2$). Then, the conditions of (14) and (20) are simply expressed by

$$C_{1,2}(k) - 2C_1(k) \geq 0, \quad C_{1,2}(k) - 2C_1(k) < 0. \quad (26)$$

Specifically, in the case of macro-diversity, the boundary condition in (25) is given by

$$\gamma_2 = \frac{(1 + 4\gamma_1)^{1/2} - 1}{2}, \quad (27)$$

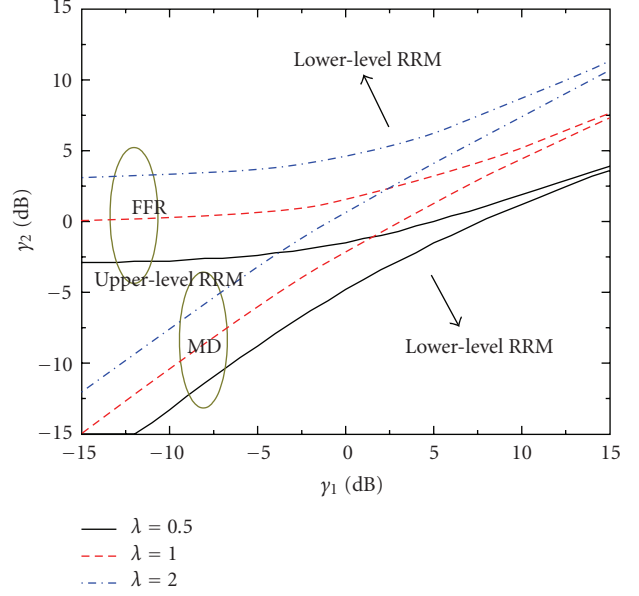


FIGURE 5: Boundary conditions of switching a RRC.

which provides an insight for designing *H_Add Threshold* and *H_Delete Threshold* for macrodiversity hand-off procedure defined in the IEEE 802.16e standard [18]. The IEEE 802.16e standard introduces a macro diversity hand-off procedure where a mobile user is able to transmit or receive unicast messages and traffic from multiple BSs at the same time interval. According to [18], when the long-term SINR of a serving BS is less than *H_Delete Threshold*, the mobile station shall send MOB_MSHO-REQ to require dropping this serving BS from the diversity set, and when the long-term SINR of a neighboring BS is higher than *H_Add Threshold*, the mobile station shall send MOB_MSHO-REQ to require adding this neighbor BS to the diversity set.

6. Implementation Issue

The overhead of RRC switch is the exchange of signaling messages for switch request and response between two RRCs. If the algorithms are triggered more frequently, the classification will probably be more accurate, but the overhead will be higher. The overhead is related to how frequently $C_1(k)$, $C_{1,2}(k)$, \bar{C}_1 , and \bar{C}_2 in (14) change.

One factor that affects a user's capacity, that is, $C_1(k)$ and $C_{1,2}(k)$ as well as \bar{C}_1 and \bar{C}_2 , is user mobility, because the capacity of fast-moving users may vary in a small-time scale. If they are able to compute γ_1 and γ_2 via a long-term average, they will not suffer from frequent RRC switch. An alternative is to make fast-moving users always be managed by the upper RRC regardless of whether they are classified as cell-interior or cell-edge users.

Meanwhile, a factor that affects \bar{C}_1 or \bar{C}_2 is addition or deletion of a user in the cell, which may trigger switching of other users. This is explained by simultaneous switching. In case more than two users trigger switching simultaneously, the conditions of a permissible switching is also derived.

TABLE 1: Parameters for simulation [19].

Channel bandwidth	5 MHz	No. of subchannels	8
Carrier frequency	2.3 GHz	TX power at BSs	43 dBm
Cell radius	1 Km	Path loss exp.	4
Shadowing var.	8 dB	Max. Doppler vel.	3 Km/hr
Number of users	30	$T_{\min}(i)$	150 Kbps
Simulation time	60 seconds	No. of simulations	1000

We refer to the set of all users for which reclassification is permissible as the permissible set. We can adopt a *sequential* approach where the user from the permissible set which offers the highest throughput gain upon switching is selected and reclassified. The permissible set is then recomputed before switching the next selected user. In each step, the procedure is the same as the reclassification algorithm stated earlier. This approach will converge to a state for which the permissible set is empty, because at each step, the system throughput strictly increases upon switching.

7. Simulation Results

We evaluated the performance in an OFDMA-based wireless network by simulation experiments, emulating mobile WiMAX systems with parameters listed in Table 1. We consider a single omnidirectional antenna at each transmitter and each receiver. In our simulator, users are uniformly distributed in a hexagonal cell and BSs of 6 first-tier and 12 second-tier neighboring cells generate intercell interference to those users. Our channel model follows path loss with an exponent of 4, Gaussian shadowing with zero mean and variance of 8 dB, and Rayleigh fading. We use the Jakes' model [20] to generate frequency-selective Rayleigh fading followed by the Doppler effect with the maximum velocity of 3 Km/hr. To serve cell-interior users, BSs either adopt a round-robin (RR) scheduling algorithm or a multichannel proportional fair (PF) scheduling algorithm [21] that guarantees minimum throughput (150 Kbps for all users in our setting) [10]. It is assumed that the channel coefficients are perfectly known at the BS and the data rate is then determined by the Shannon capacity. In our simulation, each user measures the two strongest γ 's from their neighboring BSs, and the serving BS is able to coordinate with one or two of those neighboring BSs. The cell performance was computed during the simulation time of 60 seconds, after each user's RRC had been completely determined according to our algorithm.

Our simulation results show that users are appropriately classified into cell-edge and cell-interior types by our algorithms. We confirmed that (i) the first cases in Propositions 1 and 2 are generally observed, (ii) FFR and macro-diversity (MD) increase cell-edge throughput by up to 15% when $\lambda = 1$ without a loss in system throughput, and (iii) more users switch to the cell-edge type when the neighboring cell is lightly loaded.

Figure 6 plots the ratio of edge users in the cell. The cell-edge users are now divided into the users coordinated by

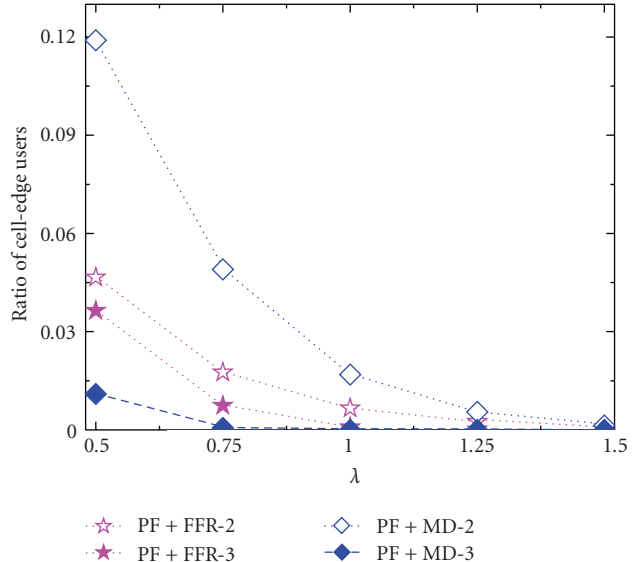


FIGURE 6: The ratio of cell-edge users for FFR-2, FFR-3, MD-2, and MD-3.

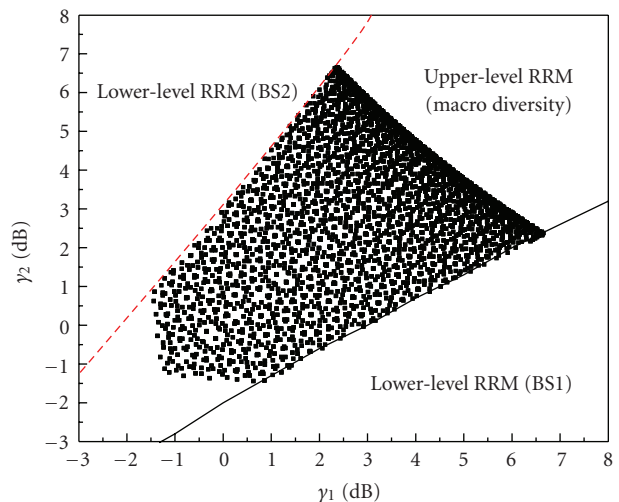


FIGURE 7: Distribution of cell-edge users' γ_1 and γ_2 when macro-diversity is used and $\bar{C}_1 = \bar{C}_2$.

two BSs (FFR-2 and MD-2) and users coordinated by three BSs (FFR-3 and MD-3). Here, PF scheduling for cell-interior users is only plotted, because RR scheduling has the same tendency. In any cases, users can take advantage of FFR-2 or MD-2 more than FFR-3 or MD-3. Interestingly, the ratio of users supported by MD-3 is very small unlike MD-2, which means that macro-diversity by three BSs is not so beneficial in enhancing the throughput of cell-edge users.

Figure 7 shows the distribution of cell-edge users' γ_1 and γ_2 in the case of Figure 5, when macro-diversity by at most two BSs is employed and $\bar{C}_1 = \bar{C}_2$. The black area represents γ_1 and γ_2 of those users by simulation results and two lines represent the threshold given by (14). In this experiment, the other cases except the first one in Propositions 1 and 2 are rarely observed; for instance, the ratio of such cases

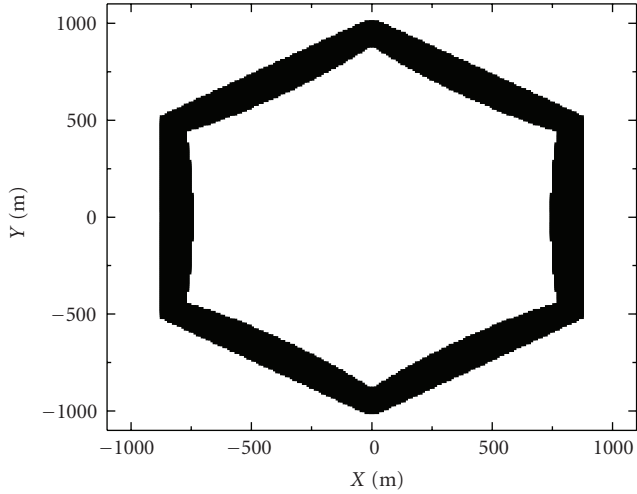


FIGURE 8: An example: the region of cell-edge users in a cell.

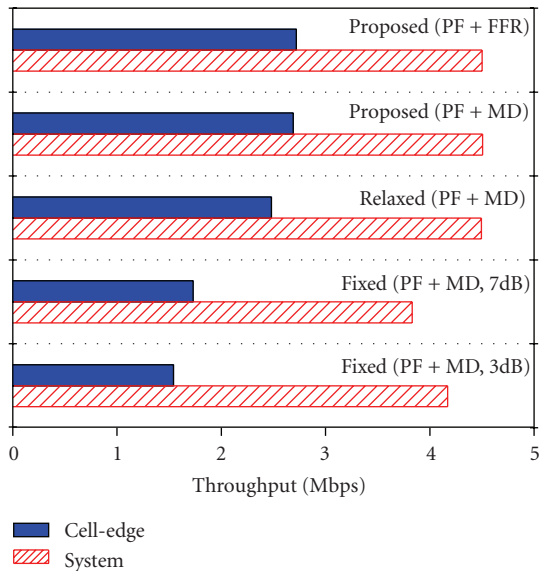


FIGURE 9: Comparison of cell-edge users’ average throughput and system throughput in various mechanisms.

is only 0.5% among all users at $\lambda = 0.2$ and it approaches zero as λ increases above 0.2. Therefore, as expected, the first cases can be regarded as the simplified solution in general. Furthermore, Figure 8 shows the possible location of cell-edge users in a hexagonal cell, when a user type is classified according to (26).

The average cell-edge throughput and system throughput (i.e., cell throughput in this simulation) are presented in Figure 9 when $\lambda = 1$. Both “PF + FFR” and “PF + MD” represent the cases where cell-interior users are supported by the PF scheduling and cell-edge users are supported by FFR or MD. The proposed algorithm shows better cell-edge throughput, compared to the relaxed switching (“Relaxed”) mentioned in Remark 2. Also, our algorithm is compared to a simple mechanism (represented by “Fixed”) where RRC

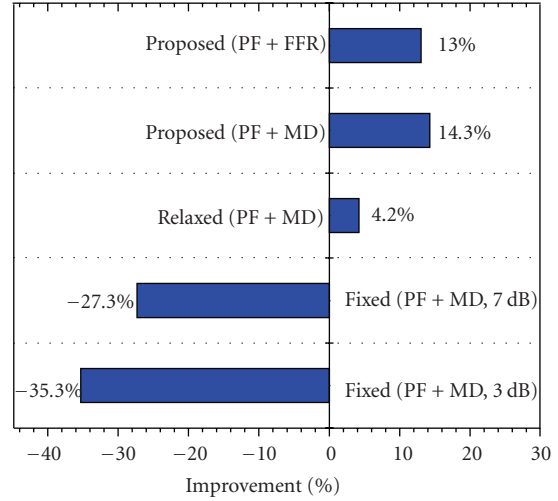


FIGURE 10: Throughput improvement of upper-managed users compared to the case with no upper RRC.

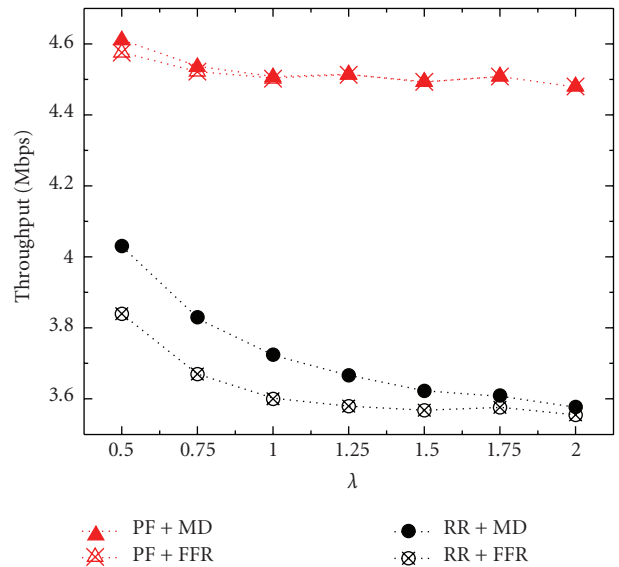


FIGURE 11: Throughput comparison between MD and FFR as a function of λ .

switch is determined by a fixed threshold, $\gamma_1 - \gamma_2$ (3 dB or 7 dB). Here, γ_2 is given by the neighboring BS that interferes most dominantly.

In the case of Figure 9, we obtained throughput improvement of cell-edge users, as shown in Figure 10. Compared to the case of no upper RRC, the proposed one improves cell-edge throughput by 13.0% and 14.3% for FFR and MD, respectively, without a loss in system throughput, while the relaxed case improves it only by 4.2%. But the “Fixed” algorithm degrades those users’ throughput. In summary, the proposed algorithm achieves the best cell-edge throughput without losing system throughput. We omit “PF + FFR” for the fixed and relaxed switching because it results in a slightly inferior cell-edge performance to “PF + MD”.

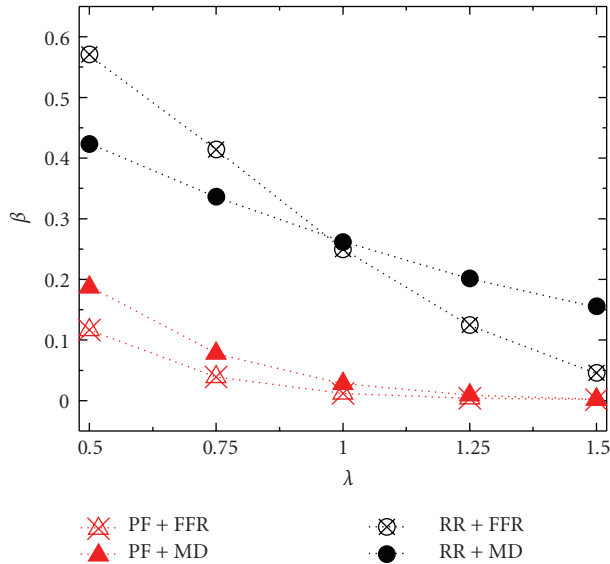
FIGURE 12: β versus λ .

Figure 11 shows the throughput comparison between FFR and MD as a function of λ , when λ is averaged over six neighboring cells. Throughput improvement decreases as λ increases, because less users are allowed to switch to the upper RRC. When PF is used for cell-interior users, there is little difference between FFR and MD. In contrast, when RR scheduling is employed for cell-interior users (see “RR + FFR” and “RR + MD”), it is shown that MD is better than FFR in improving the overall throughput.

The effect of λ is demonstrated in Figure 12 that plots β as a function of λ . Here, β also includes the fraction of resource allocated to cell-edge users who are located in six neighboring cells. As discussed in Proposition 3, users are less likely to switch to the upper RRC as λ increases. To obtain this result, we imposed no upper limit on β (i.e., $\beta_{\max} = 1$). When RR scheduling is employed for cell-interior users, they do not take advantage of opportunistic scheduling, and thus it drives more users to switch to the upper RRC. Therefore, β in case of RR scheduling is much greater than that of PF scheduling.

8. Conclusion

We have proposed a new RRM framework for wide-area wireless data networks that manages radio resources of cell-interior and cell-edge users separately. We believe that our framework can be employed with many recent approaches that require network coordination to improve cell-edge throughput, including fractional frequency reuse, macro-diversity, and various other forms of network MIMO techniques applicable to cell-edge users, although we focused on fractional frequency reuse and macro-diversity in this work. The work presented in this paper has been limited to downlink data transmission; RRM schemes for uplink in conjunction with downlink would be one avenue for future work.

Appendices

A. Proof of Proposition 1

In the case of (i), the RRC switch is possible if an $\alpha'(k)$ exists such that

$$\alpha(k) \frac{C_1(k)}{C_{1,2}(k)} \leq \alpha'(k) \leq \alpha(k) \frac{\bar{C}_1 - C_1(k)}{\bar{C}_1 + \bar{C}_2 - C_{1,2}(k)}, \quad (\text{A.1})$$

which is obtained from (10) and (11). The upper bound must be greater than the lower bound, which results in (14). The objective is maximized by the minimal value; that is, $\alpha'(k) = \alpha(k)C_1(k)/C_{1,2}(k)$. The proofs of the other cases are omitted because they follow along similar lines.

B. Proof of Proposition 3

For brevity, we only prove the case of upward switching. In the case of fractional frequency reuse, (23) is equivalent to

$$\lambda < \frac{\log(1 + \gamma_1)}{\log(1 + \gamma_1/(\gamma_2 + 1))} - 1 \triangleq f(\gamma_2) \quad (\text{B.2})$$

In the case of macro-diversity, (25) can be rewritten as

$$\lambda < \frac{1}{1 - \log(1 + \gamma_2)/\log(1 + \gamma_1 + \gamma_2)} - 1 \triangleq g(\gamma_2). \quad (\text{B.3})$$

It is easily proved that for a fixed γ_1 , $f(\gamma_2)$ and $g(\gamma_2)$ are monotonically increasing functions of γ_2 . Therefore, as the average capacity of a neighboring cell 2 increases (i.e., as λ increases), an increasing value of γ_2 is required.

Acknowledgment

Part of this paper was presented in the Proceedings of QSHINE 2009. This research was partly supported by the MKE (the Ministry of Knowledge Economy), Korea, under the ITRC (Information Technology Research Center) support program supervised by the NIPA (National IT Industry Promotion Agency) (NIPA-2009-C1090-0902-0003).

References

- [1] T.-P. Chu and S. S. Rappaport, “Overlapping coverage with reuse partitioning in cellular communication systems,” *IEEE Transactions on Vehicular Technology*, vol. 46, no. 1, pp. 41–54, 1997.
- [2] G. Li and H. Liu, “Downlink radio resource allocation for multi-cell OFDMA system,” *IEEE Transactions on Wireless Communications*, vol. 5, no. 12, pp. 3451–3459, 2006.
- [3] S.-E. Elayoubi, O. Ben Haddada, and B. Fourestié, “Performance evaluation of frequency planning schemes in OFDMA-based networks,” *IEEE Transactions on Wireless Communications*, vol. 7, no. 5, pp. 1623–1633, 2008.
- [4] Qualcomm R1-050896, “Description and simulations of interference management technique for OFDMA based E-UTRA downlink evaluation,” 3GPP TSG-RAN WG1 #42, August 2005.
- [5] S. Kim, J. Kim, D. Lim, B. C. Ihm, and H. Cho, “Interference mitigation using FFR and multi-cell MIMO in downlink,” *IEEE C802.16m-08/783r1*, July 2008.

- [6] R. C. Bernhardt, "Macroscopic diversity in frequency reuse radio systems," *IEEE Journal on Selected Areas in Communications*, vol. 5, no. 5, pp. 862–870, 1987.
- [7] M. K. Karakayali, G. J. Foschini, and R. A. Valenzuela, "Network coordination for spectrally efficient communications in cellular systems," *IEEE Wireless Communications*, vol. 13, no. 4, pp. 56–61, 2006.
- [8] G. J. Foschini, K. Karakayali, and R. A. Valenzuela, "Coordinating multiple antenna cellular networks to achieve enormous spectral efficiency," *IEEE Proceedings*, vol. 153, no. 4, pp. 548–555, 2006.
- [9] X. Liu, E. K. P. Chong, and N. B. Shroff, "Opportunistic transmission scheduling with resource-sharing constraints in wireless networks," *IEEE Journal on Selected Areas in Communications*, vol. 19, no. 10, pp. 2053–2064, 2001.
- [10] M. Andrews, L. Qian, and A. Stolyar, "Optimal utility based multi-user throughput allocation subject to throughput constraints," in *Proceedings of the Annual Joint Conference of the IEEE Computer and Communications Societies (INFOCOM '05)*, vol. 4, pp. 2415–2424, Miami, Fla, USA, March 2005.
- [11] A. Jalali, R. Padovani, and R. Pankaj, "Data throughput of CDMA-HDR a high efficiency-high data rate personal communication wireless system," in *Proceedings of the IEEE Vehicular Technology Conference (VTC '00)*, vol. 3, pp. 1854–1858, Tokyo, Japan, May 2000.
- [12] T. Yoo, N. Jindal, and A. Goldsmith, "Multi-antenna downlink channels with limited feedback and user selection," *IEEE Journal on Selected Areas in Communications*, vol. 25, no. 7, pp. 1478–1491, 2007.
- [13] 3GPP2 C.S0024-B v2.0, "cdma2000 High Rate Packet Data Air Interface Specification," April 2007.
- [14] 3GPP TR 25.858 V5.0.0, "High Speed Downlink Packet Access: Physical Layer Aspects(Release5)," March 2002.
- [15] WiMAX Forum, "WiMAX Forum Network Architecture," ver. 1.2, January 2008.
- [16] S. M. Alamouti, "A simple transmit diversity technique for wireless communications," *IEEE Journal on Selected Areas in Communications*, vol. 16, no. 8, pp. 1451–1458, 1998.
- [17] V. Tarokh, H. Jafarkhani, and A. R. Calderbank, "Space-time block codes from orthogonal designs," *IEEE Transactions on Information Theory*, vol. 45, no. 5, pp. 1456–1467, 1999.
- [18] IEEE 802.16e-2005, "Part 16: Air Interface for Fixed and Mobile Broadband Wireless Access Systems Amendment," February 2006.
- [19] WiMAX forum, "Mobile WiMAX—Part I: A Technical Overview and Performance Evaluation," August 2006.
- [20] W. C. Jakes, *Microwave Mobile Communications*, John Wiley & Sons, New York, NY, USA, 1975.
- [21] H. Kim and Y. Han, "A proportional fair scheduling for multicarrier transmission systems," *IEEE Communications Letters*, vol. 9, no. 3, pp. 210–212, 2005.